

ARTICLE

Open Access

Neuropil contraction in relation to *Complement C4* gene copy numbers in independent cohorts of adolescent-onset and young adult-onset schizophrenia patients—a pilot study

Konasale M. Prasad¹, Kodavali V. Chowdari¹, Leonardo A. D’Aiuto¹, Satish Iyengar², Jeffrey A. Stanley^{1,3} and Vishwajit L. Nimgaonkar^{1,4}

Abstract

A recent report suggested *Complement 4* (*C4A*) gene copy numbers (GCN) as risk factors for schizophrenia. Rodent model showed association of *C4* with synaptic pruning suggesting its pathophysiological significance (Sekar, A. et al. (2016)). We, therefore, predicted that *C4A* GCN would be positively correlated with neuropil contraction in the human brain among schizophrenia patients showing more prominent correlations in ventral regions among young adults and dorsal regions among adolescents since neuromaturation progresses dorsoventrally. Whole-brain, multi-voxel, in vivo phosphorus magnetic resonance spectroscopy (³¹P MRS) assessed neuropil changes by estimating levels of membrane phospholipid (MPL) precursors and catabolites. Increased MPL catabolites and/or decreased MPL precursors indexed neuropil contraction. Digital droplet PCR-based assay was used to estimate *C4A* and *C4B* GCN. We evaluated two independent cohorts (young adult-onset early-course schizophrenia (YASZ = 15) and adolescent-onset schizophrenia (AOSZ = 12) patients), and controls matched for each group, $n = 22$ and 15 , respectively. Separate forward stepwise linear regression models with Akaike information Criterion were built for MPL catabolites and precursors. *YASZ cohort*: Consistent with the rodent model (Sekar, A. et al. 2016)), *C4A* GCN positively correlated with neuropil contraction (increased pruning/decreased formation) in the inferior frontal cortex and inferior parietal lobule. *AOSZ cohort*: *C4A* GCN positively correlated with neuropil contraction in the dorsolateral prefrontal cortex and thalamus. Exploratory analysis of *C4B* GCN showed positive correlation with neuropil contraction in the cerebellum and superior temporal gyrus among YASZ while AOSZ showed neuropil contraction in the prefrontal and subcortical structures. Thus, *C4A* and *C4B* GCN are associated with neuropil contraction in regions often associated with schizophrenia, and may be neuromaturationally dependent.

Introduction

Schizophrenia is a severe brain disorder which costs over \$155 billion a year in the United States¹. Available

treatments are symptomatic leading to poor long-term social outcome^{2–5}. A better understanding of pathophysiology may help develop new treatments. One of the neurodevelopmental models that propose excessive loss of synapses⁶ may be one such mechanism. Convergent animal^{7,8}, human developmental⁹, neuroimaging^{10,11}, post-mortem^{12,13}, and computational modeling^{14,15} data suggest that increased neuropil loss predates^{16–23} and continues

Correspondence: Konasale M. Prasad (Prasadkm@upmc.edu)

¹Department of Psychiatry, University of Pittsburgh School of Medicine, Pittsburgh, PA, USA

²Department of Statistics, University of Pittsburgh, Pittsburgh, PA, USA

Full list of author information is available at the end of the article.

© The Author(s) 2018



Open Access This article is licensed under a Creative Commons Attribution 4.0 International License, which permits use, sharing, adaptation, distribution and reproduction in any medium or format, as long as you give appropriate credit to the original author(s) and the source, provide a link to the Creative Commons license, and indicate if changes were made. The images or other third party material in this article are included in the article's Creative Commons license, unless indicated otherwise in a credit line to the material. If material is not included in the article's Creative Commons license and your intended use is not permitted by statutory regulation or exceeds the permitted use, you will need to obtain permission directly from the copyright holder. To view a copy of this license, visit <http://creativecommons.org/licenses/by/4.0/>.

after the onset of psychosis^{24,25}, and may predict short-term outcome²⁶. The genetic underpinnings of excessive synaptic pruning are poorly understood in humans.

Recently, independent lines of evidence suggest that *Complement 4 (C4A)* gene copy numbers (GCN) are associated with schizophrenia risk and synaptic pruning. This is important because a number of prior studies reported altered peripheral blood complement protein levels in schizophrenia but the results were inconsistent^{27–36} and the pathophysiological significance of such alterations was unclear since the peripheral complement proteins may not cross blood brain barrier³⁷.

Persuasive results from a study by Sekar et al. (2016)³⁸ demonstrated that a copy number variant (CNV) accounts for a portion of the risk in Human Leukocyte Antigen (HLA) region reported repeatedly in genetic association studies of schizophrenia^{39–42}. This CNV consists of ‘cassettes’, denoted by ‘R-C-C-X’ that comprises *STK19 (RPI)*, *C4 (C4A or C4B)*, *CYP21A1* or *CYP21A2*, and *TNXB*⁴³. The *C4* sequences can encode *C4A* or *C4B*, which are isotypes of *C4* with > 99% sequence homology; however, the translational products differ in antigen affinities and hemolytic activity^{44–46}. A recombination site at *CYP21A2* leads to mono-, bi-, and tri-modular RCCX cassettes (and rarely, 4 modules) that can generate multiple functional copies of *C4A/C4B*, while retaining just one functional copy of the remaining genes⁴⁷. Thus, each chromosome commonly has 1–3 functional copies of *C4A/C4B*, (rarely, 0 or 4 copies), for a typical total of 0–6 copies/individual; further, transcription of *C4A/C4B* can be impacted by an intronic human endogenous retroviral (HERV) sequence⁴⁸. Sekar et al.³⁸ found that *C4A*, but not *C4B* GCN are associated with higher risk for schizophrenia. In post-mortem brain samples of schizophrenia patients, the expression of *C4A* and *C4B* genes was proportional to the number of *C4* GCN with higher expression in 5 brain regions (namely the frontal cortex, cingulate cortex, parietal cortex, cerebellum, corpus callosum and orbitofrontal cortex) by approximately 40% among schizophrenia patients compared to controls³⁸. A rodent model showed decreased synaptic pruning in *C4*-deficient mice. The RCCX CNV is also associated with risk for auto-immune disorders that have altered prevalence among schizophrenia patients^{44,49,50}. Recently, *C4* mRNA levels in plasma have been correlated with severity of psychopathology in schizophrenia⁵¹. Another study found correlations between predicted *C4A* transcription and impairment in memory⁵². Complement proteins were also associated with risk for schizophrenia⁵³, and with thinning of superior frontal cortex⁵⁴. Thus, in humans, the complement system serves diverse immune and neural functions^{55,37} and suggest that abnormal *C4A* function contributes to schizophrenia pathogenesis.

We examined the relationship of *C4* GCN with neuropil contraction/expansion in a human context within two independent cohorts of schizophrenia patients and healthy controls (HC). We examined neuropil because direct examination of synapses in live human subjects is challenging as the synapses are embedded in the neuropil. Neuropil is a synaptically dense region composed of dendrites, unmyelinated axons and glial filaments with relatively few cell bodies^{56,57}. Phosphorus magnetic resonance spectroscopy (³¹P MRS) is used to assess changes in neuronal membrane expansion/contraction within the neuropil by estimating the availability of membrane phospholipid (MPL) precursors (phosphocholine, PC; phosphoethanolamine, PE) and catabolites (glycerophosphocholine, GPC; glycerophosphoethanolamine, GPE). PC, PE, GPC, and GPE can be reliably measured in the brain by ³¹P MRS⁵⁸. Specificity of these measurements to neuropil compared to gray matter measurements is supported by convergent data from animal lesion⁵⁹, cellular model⁶⁰, human postmortem⁶¹ and neurodevelopmental studies^{9,62}. Greater sensitivity for age-related changes of MPL metabolites to neuropil changes compared to gray matter metrics is provided by human developmental studies^{9,63}. Thus, ³¹P MRS that assesses molecular biochemistry of neuropil is superior to gray matter measures that represent composite physical measurement of total volume of interneurons, synapses, axonal terminals, dendritic arborization, neuronal soma, glia, microvasculature and interneuronal space^{64,65}.

The rationale for the superiority of ³¹P MRS has been described in prior publications^{9,11,62}. Briefly, synapse/dendritic spine formation and dendritic branching requires expansion of dendritic/axonal membranes. This expansion requires increased MPL synthesis, with resultant increase in MPL precursor levels (PC + PE). This is supported by elevation of PC + PE at the time and site of neuropil growth spurts^{59,62}. Likewise, neuropil contraction or pruning are associated with breakdown of MPLs leading to elevated GPC + GPE, which is, also, noted at the time and site of synaptic pruning^{59,66}. Since expansion and contraction of neuronal membranes largely occurs at the dendrites and axonal endings during neuropil growth/contraction with a considerably smaller contribution from changes in neuronal soma size, glial expansion and myelin content^{67–69}, changes in MPL metabolites are thought to more specifically and sensitively index changes in axonal endings, dendritic branches and synapses.

We examined two independent cohorts—young adult-onset schizophrenia (YASZ) cohort ($n = 15$) and adolescent-onset schizophrenia (AOSZ) patients ($n = 12$)—and two HC cohorts age-matched for each group ($n = 22$ and 15, respectively). Examination of two cohorts helps replicate the findings and explore the association of *C4A* repeats with neuropil contraction in a developmental

context. We selected MRS voxels from five of the six brain regions that showed increased *C4A* and *C4B* expression in postmortem tissue³⁸. These included the frontal cortex (the dorsolateral prefrontal cortex (DLPFC), inferior frontal cortex (IFC), ventral PFC (VPFC)), cingulate cortex (anterior cingulate cortex (ACC) and posterior cingulate cortex (PCC)), parietal lobe (inferior parietal lobule (IPL), superior parietal lobule (SPL)), orbitofrontal cortex (OFC) and cerebellum but not corpus callosum because of lower signal-to-noise ratio (SNR) of ³¹P MRS data for this region. Since prior studies showed progression of brain maturation from the dorsal (e.g., temporal-parietal regions) to the ventral (e.g., prefrontal cortices) regions involving elimination of overproduced synapses that is prominent from late childhood to the third decade of life^{70–75}, we selected the superior temporal gyrus (STG) in addition to the above regions. Subcortical structures (thalamus, caudate, and ventral and dorsal hippocampus) were, also, included because these structures show continued maturation from childhood to late adulthood^{76–78}. Thus, fourteen regions were selected on both hemispheres so that we could examine neuropil alterations in regions that showed increased *C4* expression by Sekar et al., and neurodevelopmental changes in the dorsal (STG, PCC, IPL, SPL), ventral (DLPFC, ACC, OFC, IFC, VPFC) and subcortical regions.

Our primary hypothesis was that the GPC + GPE levels would be elevated with increasing *C4A* repeats in the frontal (DLPFC, IFC, VPFC), cingulate (ACC, PCC), parietal (IPL, SPL), the OFC and the cerebellum in both cohorts. We, further, hypothesized that the GPC + GPE levels would be elevated with increasing *C4A* repeats in YASZ cohort in the ventral brain regions (DLPFC, IFC, OFC, ACC, and VPFC) whereas the AOSZ would show such elevations in the dorsal regions (STG, PCC, IPL, and SPL). We predicted increased GPC + GPE in the hippocampus, caudate and thalamus in both cohorts because of protracted maturation. We investigated whether the *C4A* GCN would be associated with decreased PC + PE (MPL precursors) levels suggesting decreased neuropil expansion, and explored whether *C4B* GCN would be similarly correlated with GPC + GPE and PC + PE levels in these regions similar to *C4A* associations.

Methods

SAMPLE 1: YASZ and age-matched HC

Clinical evaluations

YASZ between 18–44 years of age with DSM-IV schizophrenia/schizoaffective disorder and ≤ 5 years of illness from the onset of psychotic symptoms were eligible to be enrolled at the University of Pittsburgh Medical Center. The diagnosis was confirmed in a consensus meeting of experienced diagnosticians⁷⁹ after reviewing the Structured Clinical Interview for DSM diagnosis (SCID-IV)⁸⁰

and clinical information. Total antipsychotic dose and duration were collected. Substance abuse in the previous month or dependence 6 months prior to enrollment, mental retardation per DSM-IV, serious neurological/medical illnesses were exclusion criteria. After explaining the experimental procedures, informed consents were obtained from the subjects. University of Pittsburgh IRB approved the study.

Imaging procedures

Details of ³¹P MRS data acquisition and processing are published¹¹. Briefly, whole-brain, multi-voxel, in vivo ³¹P MRS data in 3-dimensions was collected on a 3 T Siemens Tim Trio system using a dual-tuned ¹H-³¹P volume head coil and a conventional chemical shift imaging (CSI) sequence. Acquisition parameters were: FOV = 310 × 310 × 160 mm, acquired phase-encoding steps = 14 × 14 × 8 and zero-filled to 16 × 16 × 8 (nominal voxel dimension = 1.94 × 1.94 × 2.0 cm³), TR = 0.54 sec, flip-angle = 33° reflecting the Ernst angle where the average T₁ value of phosphocreatine (PCr), PE, PC was 3 sec, complex data points = 2048, spectral bandwidth = 4.0 kHz, 24 averages of the CSI matrix in which the averaging was weighted to the central k-space points conforming to a 3D elliptical function and pre-acquisition delay of 1.4 ms. T₁-weighted MPRAGE images were collected and used to guide the extraction of ³¹P MRS signal of hypothesized voxels-of-interest using an innovative procedure⁸¹. In the *k*-space domain of the ³¹P MRS data, a 75% Hamming window was applied, and modeled in the time domain with 23 Gaussian-damped sinusoids (PE, PC, GPE, and GPC as triplets, Pi, MPL_{broad}, PCr and dinucleotides as singlets, and adenosine triphosphate (ATP) (two doublets and a triplet)).

The post-processing and metabolite quantification of extracted ³¹P MRS signal was 100% automated⁸¹. Due to the *lack of ¹H decoupling*, the quantification of the individual phosphomonoesters (PE and PC), and phosphodiester (GPE and GPC) were indistinguishable. Therefore, summated measures (PE + PC, GPE + GPC) were obtained. The proportion of gray and white matter, and CSF/extra-cortical space was estimated for each voxel-of-interest using a fully automated procedure^{82–84}. Since the CSF concentration of ³¹P metabolites is below the detection limit and the ³¹P metabolites are expressed as a percentage relative to the total signal, the correction for CSF fractions is not applicable and do not confound the ³¹P MRS results.

SAMPLE 2: AOSZ and age-matched HC

Clinical evaluations

Early onset was defined as the first appearance of psychotic symptoms before 18 years of age^{85,86}. AOSZ were between 14 and 21 years of age and on stable

antipsychotic doses for longer than 1 month. SCID-IV⁸⁰ for adults and K-SADS-PL⁸⁷ for adolescents were administered and reviewed for “consensus” diagnosis as noted above. The exclusion criteria were (a) significant present/past history of medical/neurological illness, e.g., epilepsy, head injury, (b) Obstetric complications, e.g., neonatal asphyxia, (c) Mental retardation per DSM-IV, (d) Hyperbilirubinemia requiring transfusion/phototherapy > 2 days, (e) The Apgar score < 7 at 1 and 5 min after birth, (f) Gestational age < 37 or > 42 weeks, (g) Significant substance use including cigarettes > ½ pack a day, alcohol > 2 drinks/day during pregnancy, and h) Preeclampsia/eclampsia during subject’s pregnancy. These data were collected through mothers of subjects and their obstetric records. After explaining the experimental procedures, informed consents were obtained from adult subjects; subjects below 18 years of age provided the assent and then the consent was obtained from the parents or legal guardians. University of Pittsburgh IRB approved the study.

Imaging procedures

For this sample, ¹H-decoupled ³¹P MRS data was acquired. Scout images were acquired to prescribe ³¹P MRS voxels. Initial maximization of the B₀ field homogeneity in the ¹H mode (shimming) and optimization of the ³¹P reference radio frequency (RF) pulse amplitude for a 33° flip angle was conducted. The acquisition sequence includes a single slab-selective excitation RF pulse followed by phase-encoding pulses to spatially encode in 3D. The axial slab was placed parallel to the AC-PC line covering the whole brain. The scanning parameters: FOV = 310 × 310 × 160 mm, slab thickness = 140 mm, phase-encoding steps = 14 × 14 × 8, zero-filled to 16 × 16 × 8 (nominal voxel dimension = 1.94 × 1.94 × 2.0 cm³), TR = 0.54 sec, flip-angle = 33° where the average T1 value of PCr, PE, PC, is 3 sec, complex data points = 2048, spectral bandwidth = 4.0 kHz, 24 averages (weighted-average k-space), which are validated⁸⁸, elliptical k-space sampling. To minimize the signal attenuation due to spin-spin relaxation plus T2* within the pre-acquisition delay time, the rise and fall time parameters and duration of the phase encoding pulses are reduced giving a pre-acquisition delay of 1.4 ms. T1 images were acquired to shift voxels. Post-processing and quantification was similar to the non-decoupled data.

Genetic assays

Subjects were chosen randomly from the larger YASZ and AOSZ cohorts for genetic assays. Characterization of *C4* variants is challenging due to complex linkage disequilibrium in the HLA region and the complexity of *C4* locus. We used digital droplet PCR (ddPCR)³⁸ assay to estimate copy numbers of *C4* structural elements (*C4A*,

C4B, *C4L*, and *C4S*). Briefly, AluI-digested genomic DNA was mixed with primer-probe mix for *C4* and a reference locus (RPP30), and 2 × ddPCR Supermix for Probes (Bio-Rad). The oligonucleotide primers and probes used for assaying copy number of *C4A*, *C4B*, *C4L*, and *C4S* were synthesized (IDT tech), and the master mix was emulsified into droplets, using a micro-fluidic droplet generator (Bio-Rad) that was subjected to PCR. After PCR, the fluorescence in each droplet was read using a QX100 droplet reader (Bio-Rad), and the data analyzed using the QuantaSoft software (Bio-Rad) and copy numbers deduced.

To discriminate the compound structural forms of *C4* (AL, AS, BL, BS), we amplified a 5.2 kb product that spans the *C4A/B* by long-range PCR. The diluted 5.2 kb PCR product was further PCR amplified with primers specific for *C4AS* and *C4BS*. The ratio of *C4AS* to *C4BS* was used to determine *C4AS* and *C4BS* copy numbers.

Statistical analysis

We used Student’s *t* tests to examine differences in age, and χ^2 or Fisher’s exact tests to examine distribution of sex and *C4* GCN between schizophrenia and controls. Since the number of univariate tests (2 sides × 2 metabolites × 14 regions) would overwhelm hypothesis testing in this relatively small sample, we used multivariate linear modeling within SPSS 25 controlling for age and sex that would require one model for each group. Multivariate models would also account for correlation among the MPL metabolites in the hypothesized regions. Separate regression models were built for GPC + GPE and PC + PE levels for AOSZ and YASZ by including these metabolite levels for all hypothesized regions, diagnosis, age, sex and education as covariates. Since antipsychotic dose did not significantly contribute to MPL metabolite alterations¹¹, we did not covary for medications. To test primary hypothesis on the association of GPC + GPE levels with *C4A* GCNs, we built two separate forward stepwise regression models with Akaike Information Criterion (AIC) for the YASZ and the AOSZ cohorts. Smallest AIC was used to guide model selection. The AIC was used as an additional parameter because it penalizes model complexity, similar to other criterion such as Bayesian Information Criterion. We followed a similar approach to test the secondary hypothesis on the relationship of *C4A* repeats with PC + PE, and to explore the association of *C4B* repeats with GPC + GPE and PC + PE levels.

Results

Demographic and clinical characteristics

Sample 1: YASZ and age-matched HC

Although the eligibility of subjects to enter the study was 18–44 years, mean age of enrolled YASZ (25.74 ± 8.46 years) did not differ from HC (27.07 ± 7.14 years) ($t = 0.52$,

$p = 0.61$) (range 18.24 to 43.98 years for YASZ, and 18.60 to 42.10 years for HC with 3 subjects above 35 years in both groups). Mean duration of illness was 2.37 ± 1.62 years. *C4A* (Fisher's exact test, $p = 0.69$) and *C4B* (Fisher's exact test, $p = 0.23$) GCN did not show schizophrenia-HC differences (Table 1). We recapitulated our earlier published results on differences in MPL metabolites in a larger YASZ and HC cohort¹¹.

The quality of MRS data was measured as SNR, mean Gaussian linewidths of PCr and Cramer-Rao Lower Bound (CRLB) values. Gaussian linewidth of PCr represents the resolution of spectra, where narrower linewidths indicate higher resolution of spectra, and lower CRLB value is the lower bound on the variance of spectral measurements. Our larger cohort, published previously, did not show case-control differences in the mean SNR and mean Gaussian linewidths of PCr, and CRLB values for the PC + PE and GPC + GPE¹¹. This sample that was derived from the larger cohort¹¹ showed significant differences for PCr Gaussian linewidth for left caudate, hippocampus, DLPFC, thalamus, and the right ACC, IFC and caudate (all $p < 0.05$). However, the CRLB and the SNR values did not differ between the groups for these regions except for the CRLB of GPC + GPE of the left hippocampus ($p = 0.028$).

Sample 2: AOSZ and age-matched HC

Age at onset of psychosis in the AOSZ was 15.60 ± 0.8 years. Age at scan was not significantly different between

AOSZ ($n = 12$; 19.59 ± 1.60 years) and HC ($n = 15$; 19.16 ± 1.29 years) ($t = 0.76$, $p = 0.47$). AOSZ were significantly younger than YASZ ($t = 2.74$, $d. f = 25$, $p = 0.011$) (range 15.33 to 20.92 in both groups). We did not observe AOSZ-HC differences in *C4AL* (Fisher's exact test, $p = 1.00$) and *C4BL* (Fisher's exact test, $p = 0.27$) distribution in this sample, as well (Table 1).

Quality of the ¹H-decoupled ³¹P MRS was high providing improved spectral resolution and peak separation to enable clear separation of PE, PC, GPC, and GPE. The mean SNR of PCr, the mean Gaussian linewidths of the PCr and the CRLB for the PC, PE, GPC, and GPE did not show significant case-control differences except for the CRLB of PC and GPC of the left ventral hippocampus ($p = 0.025$), and the CRLB of PE of the right anterior cingulate ($p = 0.037$). These regions did not show differences associated with *C4* GCN.

C4A variants and MPL metabolites

Sample 1: YASZ and age-matched HC

In the combined sample of YASZ and HC, increasing *C4A* GCN were associated with elevated GPC + GPE levels in the ACC while IFC showed a concurrently decreased GPC + GPE and PC + PE levels. The smallest AIC for model selection was -46.20 for GPC + GPE and -43.69 for PC + PE.

Among YASZ, increasing *C4A* GCN was associated with elevated GPC + GPE levels in a ventral brain region, namely the right IFC with a large effect size (Cohen's $d =$

Table 1 Demographic and clinical characteristics

	Young adult-onset schizophrenia ($n = 15$)	Healthy controls ($n = 22$)	Statistics	Adolescent-onset schizophrenia ($n = 12$)	Healthy controls ($n = 15$)	Statistics
Age (in years)	$25.74 \pm 8.46^*$	$27.07 \pm 7.14^*$	$t = 0.52$, $p = 0.61$	$19.59 \pm 1.52^*$	$19.16 \pm 1.32^*$	$t = 0.76$, $p = 0.47$
Sex						
Male	11	5	Fisher's exact test, $p = 0.006$	10	7	Fisher's exact test, $p = 0.11$
Female	4	17		2	8	
<i>C4AL</i> repeats						
1 copy	4	4	Fisher's exact test, $p = 0.69$	1	2	Fisher's exact test, $p = 1.00$
2 or more copies	11	18		11	13	
<i>C4BL</i> repeats						
0 copy	8	15	Fisher's exact test, $p = 0.23$	7	4	Fisher's exact test, $p = 0.27$
1 copy	5	2		4	9	
2 or more copies	2	5		1	2	
Duration of illness (in years)	2.37 ± 1.62	–	–	3.99 ± 0.90	–	–

Table 2 Association of C4AL copy number repeats with MPL metabolite levels among young adult-onset schizophrenia (YASZ) and matched healthy controls

	GPC + GPE ↑	GPC + GPE ↓	PC + PE↑	PC + PE↓
Sample 1: Young adult-onset schizophrenia and age-matched HC				
YASZ + HC	L. Anterior Cingulate Cortex (AIC = -45.70; β = 0.45, t = 2.62, p = 0.013) (d = 0.43)	L. Inferior Frontal Cortex (AIC = -43.48; β = -0.27, t = 3.48, p = 0.001) (d = 0.57)		L. Inferior Frontal Cortex (AIC = -43.69; β = -0.11, t = 2.26, p = 0.03) (d = 0.37)
YASZ	R. Inferior Frontal Cortex (AIC = -20.73; β = 0.37, t = 3.81, p = 0.007) (d = 1.15)	R. Superior Parietal Lobule (AIC = -15.82; β = -0.58, t = 5.98, p = 0.001) (d = 1.8) L. Orbitofrontal Cortex (AIC = -23.87; β = -0.15, t = 2.83, p = 0.03) (d = 0.85)		L. Inferior Parietal Lobule (AIC = -18.06; β = -0.88, t = 3.26, p = 0.007) (d = 0.84)
HC	-	L. Inferior Frontal Cortex (AIC = -25.90; β = -0.17, t = 2.42, p = 0.026) (d = 0.52)		L. Inferior Frontal Cortex (AIC = -29.06; β = -0.17, t = 2.72, p = 0.014) (d = 0.57)
Sample 2: Adolescent-onset schizophrenia and age-matched HC				
AOSZ + HC	R. Dorsolateral Prefrontal Cortex (AIC = -44.78; β = 0.019, t = 2.40, p = 0.024) (d = 0.46)	L. Anterior Cingulate Cortex (AIC = -41.49; β = -0.088, t = 5.05, p < 0.001) (d = 0.99)		R. Thalamus (AIC = -35.54; β = -0.096, t = 2.96, p = 0.007) (d = 0.57)

Increased GPC + GPE suggest increased neuropil contraction while decreased PC + PE suggest decreased neuropil expansion

1.15) but not among HC. We, also, observed decreased GPC + GPE levels in the ventral regions among YASZ (the left OFC; Cohen's d = 0.85) and HC (left IFC; Cohen's d = 0.52); however, HC showed a concurrent decrease in the left IFC (Cohen's d = 0.57). YASZ patients showed decreased GPC + GPE levels (the right SPL; Cohen's d = 1.8) and decreased PC + PE levels (left IPL; Cohen's d = 0.84) in relation to increasing *C4A* repeats. Overall model AIC was -23.87 for GPC + GPE and -19.72 for PC + PE (Table 2; Fig. 1).

Sample 2: AOSZ and age-matched HC

Because there was one AOSZ and two controls with 1 copy of *C4A*, we examined the association of *C4A* repeats in the entire sample of AOSZ and HC. We noted elevated GPC + GPE levels in the DLPFC (Cohen's d = 0.46) but decreasing GPC + GPE levels in the left anterior cingulate with increasing *C4A* GCN.

In the same combined sample, we noted decreasing PC + PE levels in the right thalamus associated with increasing *C4A* GCN (Cohen's d = 0.57). Overall model AIC was -44.78 for GPC + GPE and -36.52 for PC + PE (Table 2; Fig. 1).

Post hoc tests for the association of C4BL repeats with MPL metabolite changes

Sample 1: YASZ and age-matched HC

Combined sample of YASZ + HC showed increased GPC + GPE levels in the left IPL with increasing *C4BL* repeats. Right ventral hippocampus showed elevated PC + PE and right DLPFC showed decreased PC + PE. The AIC for overall model selection was -77.07 for GPC + GPE and -18.13 for PC + PE. YASZ subjects showed elevated GPC + GPE levels in the cerebellar vermis and the left STG along with decreased PC + PE levels in the left IPL and OFC with increasing *C4BL* repeats. HC showed increased GPC + GPE levels in multiple regions with decreased PC + PE levels in the DLPFC and caudate.

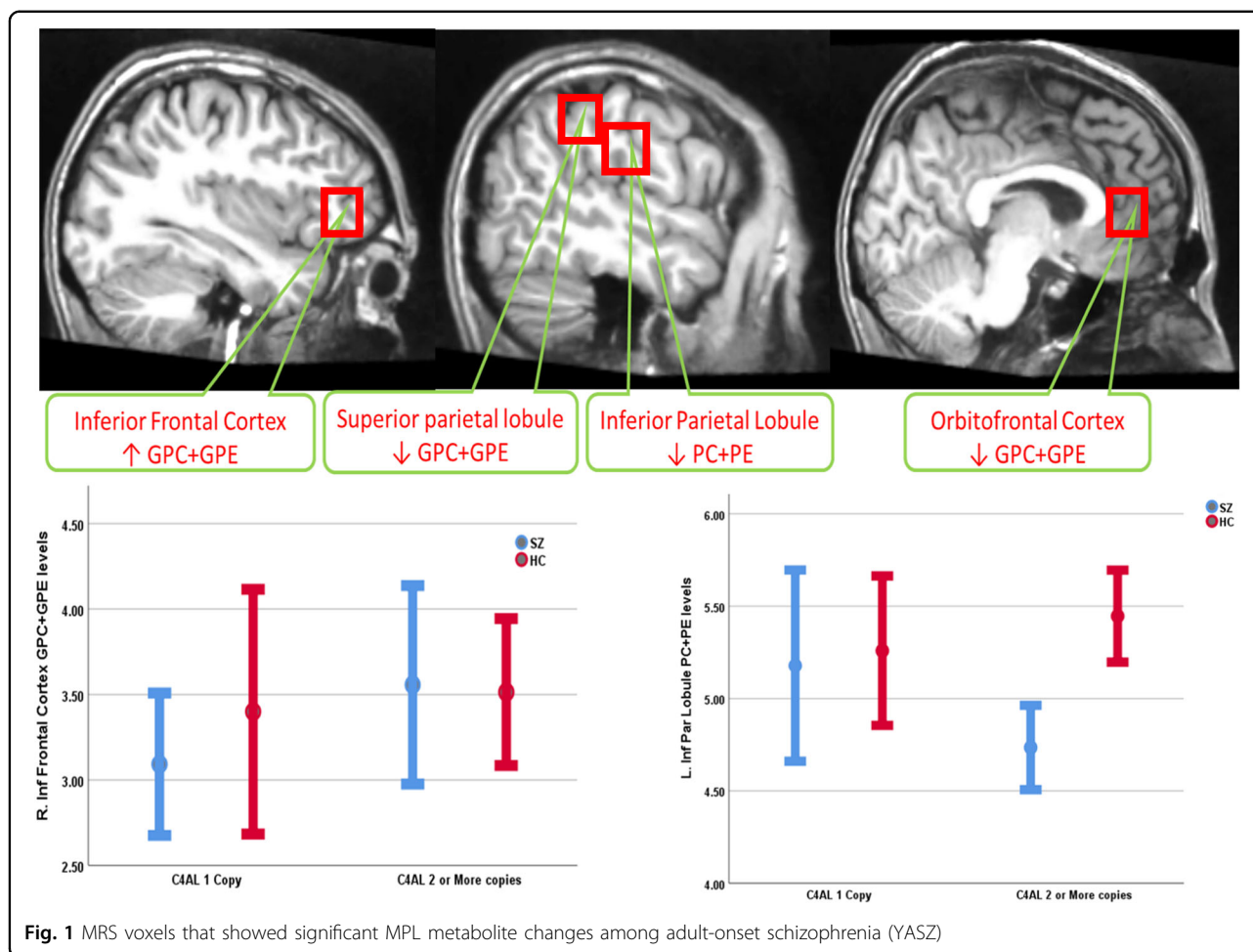
The lowest AIC for model selection was 10.92 for GPC + GPE and -13.89 for PC + PE for within YASZ and HC.

Sample 2: AOSZ and age-matched HC

Because of small n in each cell, AOSZ and HC groups were not examined separately. MPL metabolite changes in relation to *C4B* GCN were observed in the prefrontal and subcortical regions in the combined sample of AOSZ and HC. PC + PE levels did not differ between with *C4BL* repeats (Table 3; Fig. 2). AIC for overall model selection was -53.13 for GPC + GPE.

Discussion

This is the first study, to our knowledge, to demonstrate the association of *C4A* repeats with increased neuropil contraction as shown by elevated GPC + GPE levels and/or decreased PC + PE levels in two independent cohorts of schizophrenia patients. Neuropil contraction was observed in the prefrontal and parietal regions among adult-onset schizophrenia patients whereas adolescent subjects (AOSZ and controls) showed neuropil contraction in the prefrontal and thalamic regions. Our hypothesis that the GPC + GPE levels would be elevated with increasing *C4A* repeats in the frontal (DLPFC, IFC, VPFC), cingulate (ACC, PCC), parietal (IPL, SPL), the OFC and the cerebellum in both cohorts was partly supported. Our second hypothesis was, also, partly supported for the YASZ cohort in that the YASZ showed elevated GPC + GPE and/or decreased PC + PE levels in a ventral region (IFC) but not all hypothesized regions. Likewise, AOSZ + HC group showed decreased PC + PE levels in the thalamus. Overall, our results on patients and controls support the association of *C4* deficiency with synaptic pruning observed in the rodent model, although the pattern of associations are intriguing. Further, this study extends Sekar et al.³⁸ rodent model findings to human subjects with schizophrenia and for *C4B* associations with neuropil contraction although *C4B* was not associated with risk for schizophrenia.



Changes in MPL metabolite levels measured through ^{31}P MRS reflects expansion/contraction of membranes that contain the MPLs (phosphatidylcholine, PtdC; phosphatidylethanolamine, PtdE). Expansion/contraction of cell membranes that primarily occurs at the axonal endings and dendritic branches during neuropil formation/contraction are associated with elevated MPL precursors (PE, PC) and catabolites (GPC, GPE), respectively. Changes in myelination, neuronal soma size and glial cells contribute considerably less to MPL metabolite signals on ^{31}P MRS⁵⁹. Thus, major source of MPL metabolite signals is likely to be the synaptically dense neuropil^{68,69} (see our prior publication for details¹¹). Since postmortem studies have not consistently reported atrophy of neuropil⁸⁹, observed changes in MPL metabolites are unlikely to be due to general neuropil atrophy.

The first in vivo evidence of altered neuropil development in first-episode neuroleptic-naïve schizophrenia was provided by ^{31}P MRS data (decreased PC + PE and increased GPC + GPE), later supported by postmortem neuropil morphology data^{90–92}. Neuropil reduction may be linked to dendritic spine loss^{91,93–95} and decreased

neuronal soma size^{96,97} as observed in postmortem brain tissue of schizophrenia patients. Since dendritic spines receive majority of cortical excitatory synapses, dendritic spine loss may suggest loss of cortical excitatory synapses. Thus, the association of *C4A* repeats with neuropil contraction may support synaptic pruning in the rodent model³⁸. However, other factors may also contribute to neuropil reduction, e.g., peripheral blood inflammatory mediators C-reactive protein (CRP) and Interleukin-6 (IL-6) levels¹¹ but unlikely to be due to long-term administration of antipsychotics. Association of changes in MPL metabolites with antipsychotic medications has been examined in several studies. These studies show that MPL metabolites were altered with short-term but not long-term treatment^{98–101}. Given short duration of illness of both cohorts and lack of association of medications with MPL metabolites, antipsychotics may not have contributed a major variance to MPL metabolite differences in this study. Therefore, genetic influence of a variant that showed genome-wide significance on neuropil changes exemplify an attempt to explore in vivo biological significance of such variants.

Table 3 Exploratory analysis of association of C4BL copy number repeats with MPL metabolite levels among young adult-onset schizophrenia (YASZ) and matched healthy controls, and a combined sample of AOSZ + HC

	GPC + GPE↑	GPC + GPE↓	PC + PE↑	PC + PE↓
Sample 1: Young adult-onset schizophrenia and age-matched HC				
YASZ + HC	<i>L. Inferior Parietal Lobule</i> (AIC = -32.32; β = 0.32, t = 3.43, p = 0.002) (d = 0.56)	-	<i>R. Vent Hippocampus</i> (AIC = -17.92; β = 0.25, t = 2.31, p = 0.027) (d = 0.38)	<i>R. Dorsolateral Prefrontal Cortex</i> (AIC = -19.50; β = -0.38, t = 2.65, p = 0.012); (d = 0.44)
YASZ	<i>Cerebellar Vermis</i> (AIC = -9.64; β = 0.42, t = 2.69, p = 0.02) (d = 0.69)	-	<i>L. Inferior Parietal Lobule</i> (AIC = -13.44; β = 0.91, t = 3.37, p = 0.006) (d = 0.87)	-
	<i>L. Superior Temporal Gyrus</i> (AIC = -10.89; β = 0.48, t = 2.60, p = 0.025) (d = 0.67)	-	<i>L. Orbitofrontal Cortex</i> (AIC = -10.25; β = 0.18, t = 2.74, p = 0.019) (d = 0.71)	-
HC	<i>L. Superior Parietal Lobule</i> (AIC = -18.04; β = 1.86, t = 37.20, p < 0.001) (d = 7.93)	<i>L. Superior Temporal Gyrus</i> (AIC = -30.15; β = -1.05, t = 31.78, p < 0.001) (d = 6.77)	<i>Posterior Cingulate Cortex</i> (AIC = -12.43; β = 0.55, t = 3.45, p = 0.003) (d = 0.73)	<i>R. Dorsolateral Prefrontal Cortex</i> (AIC = -10.78; β = -0.38, t = 3.50, p = 0.003) (d = 0.75)
	<i>Posterior Cingulate Cortex</i> (AIC = -15.18; β = 1.42, t = 31.15, p < 0.001) (d = 6.61)	<i>L. Dorsolateral Prefrontal Cortex</i> (AIC = -15.18; β = -0.74, t = 25.72, p < 0.001) (d = 5.41)	<i>L. Hippocampus</i> (AIC = -18.13; β = 0.37, t = 2.37, p = 0.031) (d = 0.50)	<i>R. Caudate</i> (AIC = -15.36; β = -0.71, t = 3.40, p = 0.004) (d = 0.73)
	<i>L. Caudate</i> (AIC = -41.64; β = 0.45, t = 12.31, p < 0.001) (d = 2.61)	<i>L. Dorsal Hippocampus</i> (AIC = -46.70; β = -0.65, t = 13.34, p < 0.001) (d = 2.87)	-	-
	<i>L. Ventral Hippocampus</i> (AIC = -74.51; β = 0.08, t = 4.74, p = 0.001) (d = 1.00)	<i>R. Anterior Cingulate Cortex</i> (AIC = -37.77; β = -0.26, t = 12.57, p < 0.001) (d = 2.63)	-	-
Sample 2: Adolescent-onset schizophrenia and age-matched HC				
AOSZ + HC	<i>R. Caudate</i> (AIC = -34.93; β = 0.16, t = 10.07, p < 0.001) (d = 1.95)	<i>R. Thalamus</i> (AIC = -37.35; β = -0.14, t = 6.68, p < 0.001) (d = 1.26)	-	-
	<i>R. Hippocampus</i> (AIC = -34.92; β = 0.16, t = 8.07, p < 0.001) (d = 1.56)	<i>R. Anterior Cingulate Cortex</i> (AIC = -42.36; β = -0.03, t = 5.27, p < 0.001) (d = 1.09)	-	-
	<i>R. Dorsolateral Prefrontal Cortex</i> (AIC = -49.12; β = 0.03, t = 6.21, p < 0.001) (d = 1.19)	<i>L. Dorsolateral Prefrontal Cortex</i> (AIC = -41.64; β = -0.03, t = 2.18, p = 0.046) (d = 0.44)	-	-
	<i>Ventral Prefrontal Cortex</i> (AIC = -46.07; β = 0.04, t = 5.50, p < 0.001) (d = 1.03)	-	-	-
	<i>L. Orbitofrontal Cortex</i> (AIC = -34.93; β = 0.03, t = 5.34, p < 0.001) (d = 1.01)	-	-	-
	<i>L. Hippocampus</i> (AIC = -34.93; β = 0.09, t = 2.95, p = 0.011) (d = 0.56)	-	-	-

Increased GPC + GPE suggest increased neuropil contraction while decreased PC + PE suggest decreased synapse expansion

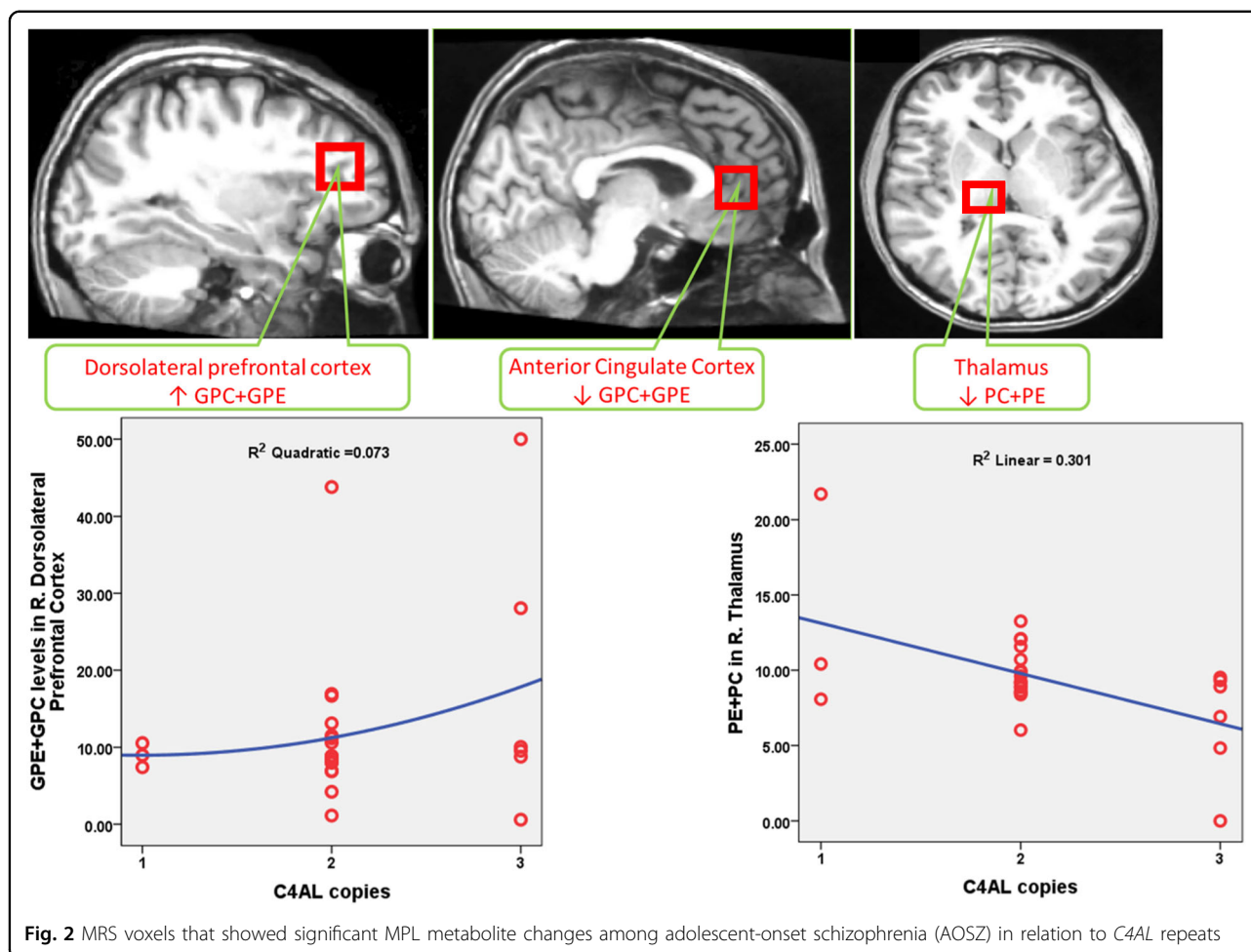


Fig. 2 MRS voxels that showed significant MPL metabolite changes among adolescent-onset schizophrenia (AOSZ) in relation to *C4AL* repeats

Among six brain regions that showed increased *C4A* and *C4B* RNA expression associated with *C4* repeats in postmortem brain tissue of schizophrenia patients³⁸, we found neuropil alterations associated with *C4A* GCN in four of five regions examined. While the frontal (DLPFC and the IFC) and parietal (IPL) regions showed increased neuropil contraction, the ACC and the OFC showed decreased neuropil contraction without altered neuropil formation. HC showed decreased neuropil turnover in the IFC. Further, the thalamus (that was not examined in the previous postmortem study³⁸) showed decreased neuropil formation in the AOSZ + HC cohort. Cerebellum did not show neuropil contraction associated with higher *C4A* GCN. Taking our in vivo ³¹P MRS data with the published data on increased RNA expression in these regions suggests that abnormal function of *C4* GCN contributes to neuropil changes in schizophrenia. However, YASZ showed variations in widespread cortical regions with greater heterogeneity in neuropil contraction/expansion compared to HC. Precise reasons for such heterogeneous

associations are unclear. Data on differential expression of *C4A* in various regions of the brain within the context of illness course or neurodevelopment are not available. Examination of whole brain ³¹P MRS data allowed us to identify brain regions beyond those examined in the postmortem study that suggests that *C4AL* may be associated with decreased neuropil synthesis, as well as neuropil contraction, both of which may be observed as dendritic spine loss—a proxy measure of synaptic pruning in postmortem studies. In the combined AOSZ + HC sample, *C4AL* showed neuropil changes in the ventral and subcortical regions. Partial support for both hypothesis may possibly be because our YASZ were not in the third decade and AOSZ were not in early adolescence where the neurodevelopment would be more active such as in early to mid-adolescence. Future postmortem and animal studies should examine these issues.

Furthermore, since the AOSZ cohort was significantly younger than the YASZ, our prediction that the AOSZ and YASZ would show regionally distinct patterns of MPL

metabolite changes in relation to *C4* GCNs broadly reflecting neurodevelopmental trajectory was not supported. This may be because the age at scan was about 19 years and the neurodevelopment might have progressed beyond dorsal regions into the ventral regions. Another reason may be inadequate power of our sample size to detect such differences. Further studies are needed to investigate developmental effects of *C4A* and *C4B* repeats.

We did not observe increased neuropil contraction among young adult HC although a concurrent reduction in PC + PE and GPC + GPE was observed in relation to *C4AL*. Exploratory analysis on the association of *C4BL* with MPL metabolites showed significant associations with increased neuropil contraction among young-adult HC compared to YASZ patients. Precise reasons are unclear; however, it is possible that the pattern of expression of *C4A* and *C4B* proteins may be different in patients compared to healthy subjects.

This study supported our secondary hypothesis of decreased neuropil expansion. It can be postulated that *C4* GCN may affect each brain region through increased neuropil contraction or decreased formation. Although postmortem examination allows direct examination of spines, differentiation of decreased spine formation from increased pruning by cross-sectional examination is challenging. Unique advantage of in vivo MRS data is its ability to distinguish between increased contraction and diminished formation to the neuropil density. Thus, the findings of this study, if replicated, raises the possibility of the contribution of *C4* GCN to decreased neuropil formation for future cellular and animal studies.

C4BL GCN were associated with MPL metabolite changes in the dorsal and subcortical regions among adult-onset schizophrenia patients. However, controls showed a similar pattern but in a distinct set of regions and were more extensive compared to patients. The associations were noted in the ventral and subcortical regions among adolescent cohort contrary to our predictions. One likely reason is that nearly half of subjects in both groups did not have any copies of *C4BL*, effectively making it a comparison between subjects with and without *C4BL* GCN. Further studies with larger samples are required.

The quality of the spectral data acquired with (AOSZ) and without (YASZ) ^1H -decoupling was reasonably good, although the ^1H -decoupled MRS data was expectedly of higher quality. The SNR and CRLB values of ^{31}P MRS data without decoupling did not show significant differences but the PCr Gaussian linewidth was longer for selected voxels suggests that the variability among the groups was within reasonable limits. The higher quality of ^1H -decoupled data suggests that higher strength magnets may be able to offer better peak separation and quantification of spectral components.

The strengths of our study include examination of two independent schizophrenia cohorts and HC groups matched for each group that shows consistency of association of *C4A* repeats with neuropil contraction, and extends the findings to decreased neuropil formation. Examining ^{31}P MRS data acquired with and without ^1H -decoupling show predicted associations with neuropil contraction supporting robustness of the findings. Innovative ddPCR assays with excellent quality control adds to these strengths. Demonstrating the associations of *C4* GCN within the human context is important because *C4A* is human-specific and supplements the rodent model observations. Examining early course patients minimizes the confounds of prolonged medication exposure, illness chronicity, and comorbid illnesses and their treatment that may affect postmortem data. Limitations of our study include relatively small sample sizes. Temporal changes could not be inferred in this cross-sectional study. ^{31}P MRS data suggests changes in the neuropil that is a synaptically dense region with few cell bodies but does not directly measure changes in synapses, dendritic arborization or spine density.

In summary, our study reports association of increased contraction and decreased formation of neuropil with the GCN of *C4* variants. Although data from gene expression studies on postmortem brain tissues and animal models are persuasive, corroboration with live human patients is critical to advance the knowledge of biological significance of gene variants observed in repeatedly replicated GWA studies. Although *C4B* was not associated with schizophrenia risk in Sekar et al. study, it is likely that *C4B* may contribute to neuropil alterations that requires further studies. Larger sample sizes need to be examined to replicate our findings.

Acknowledgements

This study was funded through the National Institute of Mental Health grants MH72995, MH93540, and MH101566 (KMP), and MH63480 and the Stanley Medical Research Institute (SMRI) (V.L.N.). We thank Ms. Diana Mermon, Ms. Alicia Thomas, Ms. Karol Rosengarth, Mr. Kevin Eklund, Mr. Dhruvan Goradia, Ms. Jean Miewald and Dr. Debra Montrose in characterizing subjects and help with data management.

Author details

¹Department of Psychiatry, University of Pittsburgh School of Medicine, Pittsburgh, PA, USA. ²Department of Statistics, University of Pittsburgh, Pittsburgh, PA, USA. ³Department of Psychiatry and Behavioral Neuroscience, Wayne State University School of Medicine, Detroit, MI, USA. ⁴Department of Human Genetics, Graduate School of Public Health, University of Pittsburgh, Pittsburgh, PA, USA

Conflict of interest

The authors declare that they have no conflict of interest.

Publisher's note

Springer Nature remains neutral with regard to jurisdictional claims in published maps and institutional affiliations.

Received: 1 May 2018 Accepted: 14 May 2018

Published online: 19 July 2018

References

- Cloutier, M. et al. The Economic Burden of Schizophrenia in the United States in 2013. *J. Clin. Psychiatry* **77**, 764–771 (2016).
- Robinson, D. G., Woerner, M. G., McMeniman, M., Mendelowitz, A. & Bilder, R. M. Symptomatic and functional recovery from a first episode of schizophrenia or schizoaffective disorder. *Am. J. Psychiatry* **161**, 473–479 (2004).
- Henry, L. P. et al. The EPPIC follow-up study of first-episode psychosis: longer-term clinical and functional outcome 7 years after index admission. *J. Clin. Psychiatry* **71**, 716–728 (2010).
- Jaaskelainen, E. et al. A systematic review and meta-analysis of recovery in schizophrenia. *Schizophr. Bull.* **39**, 1296–1306 (2013).
- Modestin, J., Huber, A., Satirli, E., Malti, T. & Hell, D. Long-term course of schizophrenic illness: Bleuler's study reconsidered. *Am. J. Psychiatry* **160**, 2202–2208 (2003).
- Feinberg, I. Schizophrenia: caused by a fault in programmed synaptic elimination during adolescence? *J. Psychiatr. Res.* **17**, 319–334 (1982).
- Mayilyan, K. R., Weinberger, D. R. & Sim, R. B. The complement system in schizophrenia. *Drug. News Perspect.* **21**, 200–210 (2008).
- Meyer, U. Developmental neuroinflammation and schizophrenia. *Prog. Neuropsychopharmacol. Biol. Psychiatry* **42**, 20–34 (2013).
- Stanley, J. A. et al. Evidence of developmental alterations in cortical and subcortical regions of children with attention-deficit/hyperactivity disorder: a multivoxel in vivo phosphorus 31 spectroscopy study. *Arch. Gen. Psychiatry* **65**, 1419–1428 (2008).
- Pettegrew, J. W. et al. Alterations in brain high-energy phosphate and membrane phospholipid metabolism in first-episode, drug-naive schizophrenics. A pilot study of the dorsal prefrontal cortex by in vivo phosphorus 31 nuclear magnetic resonance spectroscopy. *Arch. Gen. Psychiatry* **48**, 563–568 (1991).
- Prasad, K. M., Burgess, A., Nimgaonkar, V. L., Keshavan, M. S. & Stanley, J. A. Neuregulin pruning in early-course schizophrenia: immunological, clinical and neurocognitive correlates. *Biol. Psychiatry: Cognitive Neuroscience & Neuroimaging* **1**, 528–538 (2016).
- Glausier, J. R. & Lewis, D. A. Dendritic spine pathology in schizophrenia. *Neuroscience* **251**, 90–107 (2013).
- Mirnic, K., Middleton, F. A., Lewis, D. A. & Levitt, P. Analysis of complex brain disorders with gene expression microarrays: schizophrenia as a disease of the synapse. *Trends Neurosci.* **24**, 479–486 (2001).
- Hoffman, R. E. & Dobscha, S. K. Cortical pruning and the development of schizophrenia: a computer model. *Schizophr. Bull.* **15**, 477–490 (1989).
- Hoffman, R. E. & McGlashan, T. H. Neural network models of schizophrenia. *Neuroscientist* **7**, 441–454 (2001).
- Cannon, T. D. et al. Progressive reduction in cortical thickness as psychosis develops: a multisite longitudinal neuroimaging study of youth at elevated clinical risk. *Biol. Psychiatry* **77**, 147–157 (2015).
- Pantelis, C. et al. Neuroanatomical abnormalities before and after onset of psychosis: a cross-sectional and longitudinal MRI comparison. *Lancet* **361**, 281–288 (2003).
- Sun, D. et al. Progressive brain structural changes mapped as psychosis develops in 'at risk' individuals. *Schizophr. Res.* **108**, 85–92 (2009).
- Takahashi, T. et al. Insular cortex gray matter changes in individuals at ultra-high-risk of developing psychosis. *Schizophr. Res.* **111**, 94–102 (2009).
- Takahashi, T. et al. Progressive gray matter reduction of the superior temporal gyrus during transition to psychosis. *Arch. Gen. Psychiatry* **66**, 366–376 (2009).
- Ziermans, T. B. et al. Progressive structural brain changes during development of psychosis. *Schizophr. Bull.* **38**, 519–530 (2012).
- Borgwardt, S. J. et al. Reductions in frontal, temporal and parietal volume associated with the onset of psychosis. *Schizophr. Res.* **106**, 108–114 (2008).
- Walter, A. et al. Hippocampal volume in subjects at high risk of psychosis: a longitudinal MRI study. *Schizophr. Res.* **142**, 217–222 (2012).
- Bangalore, S. S. et al. Untreated illness duration correlates with gray matter loss in first-episode psychoses. *Neuroreport* **20**, 729–734 (2009).
- Lieberman, J. et al. Longitudinal study of brain morphology in first episode schizophrenia. *Biol. Psychiatry* **49**, 487–499 (2001).
- Prasad, K. M., Sahni, S. D., Rohm, B. R. & Keshavan, M. S. Dorsolateral prefrontal cortex morphology and short-term outcome in first-episode schizophrenia. *Psychiatry Res.* **140**, 147–155 (2005).
- Rudduck, C., Beckman, L., Franzen, G., Jacobsson, L. & Lindstrom, L. Complement factor C4 in schizophrenia. *Hum. Hered.* **35**, 223–226 (1985).
- Mayilyan, K. R., Dodds, A. W., Boyajyan, A. S., Soghoyan, A. F. & Sim, R. B. Complement C4B protein in schizophrenia. *World J. Biol. Psychiatry.* **9**, 225–230 (2008).
- Hakobyan, S., Boyajyan, A. & Sim, R. B. Classical pathway complement activity in schizophrenia. *Neurosci. Lett.* **374**, 35–37 (2005).
- Shcherbakova, I. et al. The possible role of plasma kallikrein-kinin system and leukocyte elastase in pathogenesis of schizophrenia. *Immunopharmacology* **43**, 273–279 (1999).
- Maes, M. et al. Acute phase proteins in schizophrenia, mania and major depression: modulation by psychotropic drugs. *Psychiatry Res.* **66**, 1–11 (1997).
- Mayilyan, K. R., Arnold, J. N., Presanis, J. S., Soghoyan, A. F. & Sim, R. B. Increased complement classical and mannan-binding lectin pathway activities in schizophrenia. *Neurosci. Lett.* **404**, 336–341 (2006).
- Fananas, L., Moral, P., Panadero, M. A. & Bertranpetit, J. Complement genetic markers in schizophrenia: C3, BF and C6 polymorphisms. *Hum. Hered.* **42**, 162–167 (1992).
- Spivak, B. et al. Reduced total complement haemolytic activity in schizophrenic patients. *Psychol. Med.* **23**, 315–318 (1993).
- Idonije, O. B., Akinlade, K. S., Ihenyena, O. & Arinola, O. G. Complement factors in newly diagnosed Nigerian schizophrenic patients and those on anti-psychotic therapy. *Niger J. Physiol. Sci.* **27**, 19–21 (2012).
- Schroers, R. et al. Investigation of complement C4B deficiency in schizophrenia. *Hum. Hered.* **47**, 279–282 (1997).
- Veerhuis, R., Nielsen, H. M. & Tenner, A. J. Complement in the brain. *Mol. Immunol.* **48**, 1592–1603 (2011).
- Sekar, A. et al. Schizophrenia risk from complex variation of complement component 4. *Nature* **530**, 177–183 (2016).
- Purcell, S. M. et al. Common polygenic variation contributes to risk of schizophrenia and bipolar disorder. *Nature* **460**, 748–752 (2009).
- Ripke, S. et al. Genome-wide association study identifies five new schizophrenia loci. *Nat. Genet.* **43**, 969–976 (2011).
- Shi, J. et al. Common variants on chromosome 6p22.1 are associated with schizophrenia. *Nature* **460**, 753–757 (2009).
- Stefansson, H. et al. Common variants conferring risk of schizophrenia. *Nature* **460**, 744–747 (2009).
- Mason, M. J. et al. Low HERV-K(C4) copy number is associated with type 1 diabetes. *Diabetes* **63**, 1789–1795 (2014).
- Yang, Y. et al. Gene copy-number variation and associated polymorphisms of complement component C4 in human systemic lupus erythematosus (SLE): low copy number is a risk factor for and high copy number is a protective factor against SLE susceptibility in European Americans. *Am. J. Hum. Genet.* **80**, 1037–1054 (2007).
- Dodds, A. W., Ren, X. D., Willis, A. C. & Law, S. K. The reaction mechanism of the internal thioester in the human complement component C4. *Nature* **379**, 177–179 (1996).
- Isernman, D. E. & Young, J. R. The molecular basis for the difference in immune hemolysis activity of the Chido and Rodgers isotypes of human complement component C4. *J. Immunol.* **132**, 3019–3027 (1984).
- Blanchong, C. A. et al. Genetic, structural and functional diversities of human complement components C4A and C4B and their mouse homologues, Slp and C4. *Int. Immunopharmacol.* **1**, 365–392 (2001).
- Mack, M., Bender, K. & Schneider, P. M. Detection of retroviral antisense transcripts and promoter activity of the HERV-K(C4) insertion in the MHC class III region. *Immunogenetics* **56**, 321–332 (2004).
- Blanchong, C. A. et al. Deficiencies of human complement component C4A and C4B and heterozygosity in length variants of RP-C4-CYP21-TNX (RCCX) modules in caucasians. The load of RCCX genetic diversity on major histocompatibility complex-associated disease. *J. Exp. Med.* **191**, 2183–2196 (2000).
- Nimgaonkar, V. L., Prasad, K. M., Chowdari, K. V., Severance, E. G. & Yolken, R. H. The complement system: a gateway to gene-environment interactions in schizophrenia pathogenesis. *Mol. Psychiatry* **22**, 1554–1561 (2017).
- Melbourne J. K., Rosen C., Feiner B., Sharma R. P. C4A mRNA expression in PBMCs predicts the presence and severity of delusions in schizophrenia and bipolar disorder with psychosis. *Schizophr. Res. Epub ahead of print 2018/02/17* (2018).
- Donohoe G., et al. Genetically predicted complement component 4A expression: effects on memory function and middle temporal lobe activation. *Psychol. Med.* **48**:10:1608–1615 (2018).

53. English, J. A. et al. Blood-based protein changes in childhood are associated with increased risk for later psychotic disorder: evidence from a nested case-control study of the ALSPAC longitudinal birth cohort. *Schizophr. Bull.* **44**, 297–306 (2018).
54. Allswede, D. M. et al. Complement gene expression correlates with superior frontal cortical thickness in humans. *Neuropsychopharmacology* **43**, 525–533 (2018).
55. Ricklin, D., Reis, E. S., Mastellos, D. C., Gros, P. & Lambris, J. D. Complement component C3 - 'Swiss Army Knife' of innate immunity and host defense. *Immunol. Rev.* **274**, 33–58 (2016).
56. Kandel, E. R. in *Principles of Neural Science* 5th edn, Vol. I (McGraw-Hill, New York, 2013) 1709 pp.
57. Gazzaniga, M. S. in *The Cognitive Neurosciences* 4th edn, Vol. 17 (MIT Press, Cambridge, 2009) 1294 p.
58. Stanley, J. A., Pettegrew, J. W. & Keshavan, M. S. Magnetic resonance spectroscopy in schizophrenia: methodological issues and findings—part I. *Biol. Psychiatry* **48**, 357–368 (2000).
59. Geddes, J. W., Panchalingam, K., Keller, J. N. & Pettegrew, J. W. Elevated phosphocholine and phosphatidylcholine following rat entorhinal cortex lesions. *Neurobiol. Aging* **18**, 305–308 (1997).
60. Marucci, H., Paoletti, L., Jackowski, S. & Banchio, C. Phosphatidylcholine biosynthesis during neuronal differentiation and its role in cell fate determination. *J. Biol. Chem.* **285**, 25382–25393 (2010).
61. O'Brien, J. S. & Sampson, E. L. Lipid composition of the normal human brain: gray matter, white matter, and myelin. *J. Lipid Res.* **6**, 537–544 (1965).
62. Pettegrew, J. W., Klunk, W. E., Panchalingam, K., McClure, R. J. & Stanley, J. A. Molecular insights into neurodevelopmental and neurodegenerative diseases. *Brain Res. Bull.* **53**, 455–469 (2000).
63. Goldstein, G. et al. Molecular neurodevelopment: an in vivo 31P-1H MRSI study. *J. Int. Neuropsychol. Soc.* **15**, 671–683 (2009).
64. Eriksson, S. H. et al. Correlation of quantitative MRI and neuropathology in epilepsy surgical resection specimens—T2 correlates with neuronal tissue in gray matter. *Neuroimage* **37**, 48–55 (2007).
65. Lockwood-Estrin, G. et al. Correlating 3T MRI and histopathology in patients undergoing epilepsy surgery. *J. Neurosci. Methods* **205**, 182–189 (2012).
66. Pettegrew, J. W. et al. 31P nuclear magnetic resonance studies of phospholipid metabolism in developing and degenerating brain: preliminary observations. *J. Neuropathol. Exp. Neurol.* **46**, 419–430 (1987).
67. Palay, S. L. & Chan-Palay, V. in *Cellular Biology of Neurons*. (ed. Kandel, E. R.) 5–37 (American Physiological Society, Bethesda, 1977).
68. Pfenninger, K. H. Plasma membrane expansion: a neuron's Herculean task. *Nat. Rev. Neurosci.* **10**, 251–261 (2009).
69. Pfenninger, K. H. & Johnson, M. P. Membrane biogenesis in the sprouting neuron. I. Selective transfer of newly synthesized phospholipid into the growing neurite. *J. Cell. Biol.* **97**, 1038–1042 (1983).
70. Thompson, P. M. et al. From the Cover: Mapping adolescent brain change reveals dynamic wave of accelerated gray matter loss in very early-onset schizophrenia. *PNAS* **98**, 11650–11655 (2001).
71. Gogtay, N. et al. Dynamic mapping of human cortical development during childhood through early adulthood. *Proc. Natl Acad. Sci. USA* **101**, 8174–8179 (2004).
72. Giedd, J. N. et al. Brain development during childhood and adolescence: a longitudinal MRI study. *Nat. Neurosci.* **2**, 861–863 (1999).
73. Huttenlocher, P. R. Synaptic density in human frontal cortex—developmental changes and effects of aging. *Brain Res.* **163**, 195–205 (1979).
74. Huttenlocher, P. R. Synapse elimination and plasticity in developing human cerebral cortex. *Am. J. Ment. Defic.* **88**, 488–496 (1984).
75. Huttenlocher, P. R. & Dabholkar, A. S. Regional differences in synaptogenesis in human cerebral cortex. *J. Comp. Neurol.* **387**, 167–178 (1997).
76. Goddings, A. L. et al. The influence of puberty on subcortical brain development. *Neuroimage* **88**, 242–251 (2014).
77. Jabes, A., Lavenex, P. B., Amaral, D. G. & Lavenex, P. Postnatal development of the hippocampal formation: a stereological study in macaque monkeys. *J. Comp. Neurol.* **519**, 1051–1070 (2011).
78. Lavenex, P., Banta Lavenex, P. & Amaral, D. G. Postnatal development of the primate hippocampal formation. *Dev. Neurosci.* **29**, 179–192 (2007).
79. Stolz, E. et al. Brain activation patterns during visual episodic memory processing among first-degree relatives of schizophrenia subjects. *Neuroimage* **63**, 1154–1161 (2012).
80. First, M. B. *The Structured Clinical Interview for DSM-IV for Axis I disorders: Clinical Version, Administration Booklet*. (American Psychiatric Press, Washington, 1997).
81. Wu, H., Goradia, D. D. & Stanley, J. A. A fully automated and robust method of extracting CSI voxels from precise anatomical locations: An application to a longitudinal ³¹P MRS study. A fully automated and robust method of extracting CSI voxels from precise anatomical locations: An application to a longitudinal ³¹P MRS study. *Proceedings of the The International Society of Magnetic Resonance in Medicine* (Milan, Italy, 2014).
82. Jenkinson, M., Beckmann, C. F., Behrens, T. E. J., Woolrich, M. W. & Smith, S. M. FSL. *Neuroimage* **62**, 782–790 (2012).
83. Dale, A., Fischl, B. & Sereno, M. Cortical surface-based analysis. I. Segmentation and surface reconstruction. *Neuroimage* **9**, 179–194 (1999).
84. Fischl, B. & Dale, A. Measuring the thickness of the human cerebral cortex from magnetic resonance images. *Proc. Natl Acad. Sci. USA* **97**, 11050–11055 (2000).
85. Maziade, M. et al. Long-term stability of diagnosis and symptom dimensions in a systematic sample of patients with onset of schizophrenia in childhood and early adolescence. I: nosology, sex and age of onset. *Br. J. Psychiatry* **169**, 361–370 (1996).
86. Frangou, S., Hadjulis, M. & Vourdas, A. The Maudsley early onset schizophrenia study: cognitive function over a 4-year follow-up period. *Schizophr. Bull.* **34**, 52–59 (2008).
87. Kaufman, J., Birmaher, B., Brent, D. A., Ryan, N. D. & Rao, U. K-Sads-P. *J. Am. Acad. Child Adolesc. Psychiatry* **39**, 1208 (2000).
88. Pohmann, R. & von Kienlin, M. Accurate phosphorus metabolite images of the human heart by 3D acquisition-weighted CSI. *Magn. Reson. Med.* **45**, 817–826 (2001).
89. Harrison, P. J. The neuropathology of schizophrenia. A critical review of the data and their interpretation. *Brain* **122**, 593–624 (1999). Pt 4.
90. Selemon, L. D. & Goldman-Rakic, P. S. The reduced neuropil hypothesis: a circuit based model of schizophrenia. *Biol. Psychiatry* **45**, 17–25 (1999).
91. Glantz, L. A. & Lewis, D. A. Decreased dendritic spine density on prefrontal cortical pyramidal neurons in schizophrenia. *Arch. Gen. Psychiatry* **57**, 65–73 (2000).
92. Glantz, L. A. & Lewis, D. A. Dendritic spine density in schizophrenia and depression. *Arch. Gen. Psychiatry* **58**, 203 (2001).
93. Garey, L. J. et al. Reduced dendritic spine density on cerebral cortical pyramidal neurons in schizophrenia. *J. Neurol. Neurosurg. Psychiatry* **65**, 446–453 (1998).
94. MacDonald, M. L. et al. Selective loss of smaller spines in schizophrenia. *Am. J. Psychiatry* **174**, 586–594 (2017).
95. Sweet, R. A., Henteleff, R. A., Zhang, W., Sampson, A. R. & Lewis, D. A. Reduced dendritic spine density in auditory cortex of subjects with schizophrenia. *Neuropsychopharmacology* **34**, 374–389 (2009).
96. Sweet, R. A. et al. Pyramidal cell size reduction in schizophrenia: evidence for involvement of auditory feedforward circuits. *Biol. Psychiatry* **55**, 1128–1137 (2004).
97. Sweet, R. A., Pierri, J. N., Auh, S., Sampson, A. R. & Lewis, D. A. Reduced pyramidal cell somal volume in auditory association cortex of subjects with schizophrenia. *Neuropsychopharmacology* **28**, 599–609 (2003).
98. Smesny, S. et al. Antipsychotic drug effects on left prefrontal phospholipid metabolism: a follow-up 31P-2D-CSI study of haloperidol and risperidone in acutely ill chronic schizophrenia patients. *Schizophr. Res.* **138**, 164–170 (2012).
99. Volz, H. P. et al. Increase of phosphodiesterases during neuroleptic treatment of schizophrenics: a longitudinal 31P-magnetic resonance spectroscopic study. *Biol. Psychiatry* **45**, 1221–1225 (1999).
100. Volz, H. P. et al. 31Phosphorus magnetic resonance spectroscopy of the dorsolateral prefrontal region in schizophrenics—a study including 50 patients and 36 controls. *Biol. Psychiatry* **44**, 399–404 (1998).
101. Jayakumar, P. N. et al. High energy phosphate abnormalities normalize after antipsychotic treatment in schizophrenia: a longitudinal 31P MRS study of basal ganglia. *Psychiatry Res.* **181**, 237–240 (2010).